Acta Mechanica 187, 1–9 (2006)
DOI 10.1007/s00707-006-0375-y

Acta Mechanica
Printed in Austria

A generally applicable approximate solution for mixed mode crack-inclusion interaction

Z. Li and **Q. Sheng**, Shanghai, and **J. Sun**, Xian, China

Received February 6, 2006; revised May 12, 2006
Published online: August 3, 2006

Summary. Based on the transformation toughening theory an approximate solution is developed for predicting the stress intensity factor for a crack interacting with an inclusion of arbitrary shape and size under I/II mixed mode loading conditions. The transformation strains in the inclusion induced by the crack tip field and the remotely applied stresses are evaluated based on the Eshelby equivalent inclusion theory. As validated by detailed finite element analyses, the solution is applicable with good accuracy for the inclusion of arbitrary shape and large size under mixed mode loadings.

1 Introduction

The interaction between a crack and an inclusion has been extensively studied over years because it is evidently important for understanding the mechanisms of strengthening and toughening, material damage and fracture for composite materials discontinuously reinforced by particles or fibers. However, only a few and highly idealized cases, such as circular or elliptical inclusion, have been treated analytically due to the complexity of this kind of problems [1]–[5]. Most of the studies have been performed by numerical approaches, such as finite element method [6]–[9], boundary element method [7], [10]–[12], and singular integral equation method [13], [14]. Although these numerical analyses provide some insight into understanding interactions between crack and inclusion, these numerical results are limited to fixed calculation parameters. No generalizations could be drawn from these numerical results because of the intricacy of the results in the individual situations. Thus, the knowledge of the interaction between a crack and an inclusion comes by slow accumulation of results for special cases, rather than by establishment of general propositions.

An exacts analytical solution for the interaction between a crack and an inclusion of arbitrary configuration is very difficult to obtain from the linear theory of elasticity. Hence, an approximate analytical solution is desirable in practice. In our previous studies [15], [16], approximate solutions for mode I and mode II cracks near or partially penetrating an inclusion of arbitrary shape have been obtained based on transformation toughening theory and Eshelby equivalent inclusion theory. As validated by numerical examples, these approximate solutions have fairly good accuracy. However, although these solutions are applicable for an inclusion of arbitrary shape, the inclusion must be located in the crack tip field which is controlled by the

remotely applied stress intensity factor. Therefore, the size of the inclusion must be very small compared with the crack length. This limits the application of these solutions.

In the present study, we assume that the stress fields acting on an inclusion are approximated by superposition of the crack tip field and the remotely applied stresses. Then the transformation strains induced by I/II mixed mode crack and remotely applied stresses are evaluated based on Eshelby equivalent inclusion method, from which a generally applicable approximation solution for the interaction between the mixed-mode crack and an inclusion of arbitrary shape and size is derived based on the transformation toughening theory. It is shown that, in comparison with corresponding numerical results, the present solution has good accuracy for the inclusion of large size. When the inclusion size is small as compared with the crack length and the inclusion locates in the crack tip field, the present solution reduces to previous ones [16], [17].

2 Model and formulation

Figure 1 shows a plane structure containing a crack and an inclusion of arbitrary shape subjected to remotely applied stress σ_{ij}^0. Commonly, mode I and mode II stress intensity factors (SIFs) will be developed due to unsymmetry of the applied load and the shape of inclusion with respect to the crack line. Assume that the mode I and mode II SIFs are K_I^0 and K_{II}^0 in the absence of inclusion. The near tip SIFs will be changed due to the presence of the inclusion, denoted by K_I^{tip} and K_{II}^{tip}, respectively. The goal of the present study is to seek approximate solutions of K_I^{tip} and K_{II}^{tip} for the inclusion of arbitrary shape and size. The plane strain condition will be considered in the following.

If the elastic constants of the inclusion differ from those of the matrix material, a transformation strain $\mathbf{e}^{\mathrm{T}}$ will be induced by the crack tip stress field and the remotely applied stresses due to the inhomogeneity between matrix material and the inclusion. Now, consider a differential element dA located at (r, θ) within the inclusion. According to the Eshelby equivalent inclusion approach [18], [19], the equivalent transformation strain in dA can be expressed by

$$\mathbf{e}^{\mathrm{T}} = [(\mathbf{C}_{\mathrm{i}} - \mathbf{C}_{\mathrm{m}})\mathbf{S} + \mathbf{C}_{\mathrm{m}}]^{-\mathbf{1}}(\mathbf{C}_{\mathrm{i}} - \mathbf{C}_{\mathrm{m}})\mathbf{e}^{\mathrm{A}}, \tag{1}$$

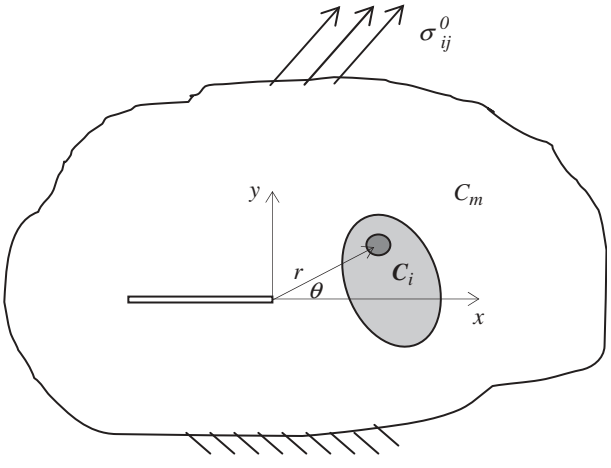

Fig. 1. The mechanical model

where $\mathbf{S}$ is the Eshelby tensor, dependent solely upon the inclusion shape and the Poisson's ratio of the matrix material. $\mathbf{C}_{\mathrm{i}}$ and $\mathbf{C}_{\mathrm{m}}$ are the elastic tensors of the inclusion and matrix material, respectively. $\mathbf{e}^{\mathrm{A}}$ is the applied strain in the absence of the inclusion. As shown in (1), the equivalent transformation strain $\mathbf{e}^{\mathrm{T}}$ in dA varies with the applied strain $\mathbf{e}^{\mathrm{A}}$, and is not zero for an inhomogeneous inclusion ($\mathbf{C}_{\mathrm{i}} \neq \mathbf{C}_{\mathrm{m}}$).

For simplicity, it is assumed that the inclusion and matrix material are isotropic and their Poisson's ratios are the same, denoted by v. Then we have

$$\mathbf{C}_{\mathrm{i}} = \alpha \mathbf{C}_{\mathrm{m}}, \tag{2}$$

where

$$\alpha = E_i/E_m. \tag{3}$$

E_i and E_m are the Young's moduli of the inclusion and matrix material, respectively.

Substituting Eq. (2) into (1) yields

$$\mathbf{e}^{\mathrm{T}} = \mathbf{L}\mathbf{e}^{\mathrm{A}}, \tag{4}$$

where

$$\mathbf{L} = [(\alpha - 1)\mathbf{S} + \mathbf{I}]^{-1}(1 - \alpha). \tag{5}$$

$\mathbf{I}$ is the unit tensor. Thus, the tensor $\mathbf{L}$ relates the equivalent transformation strain $\mathbf{e}^{\mathrm{T}}$ in the inclusion to the applied strain $\mathbf{e}^{\mathrm{A}}$ without going into the details of the form of the $\mathbf{C}_{\mathrm{i}}$ and $\mathbf{C}_{\mathrm{m}}$ tensors.

For a differential element with circular section inside the inclusion, the components of the Esbelby tensor are given by [20]

$$\begin{aligned}
&S_{1111} = S_{2222} = \frac{5 - 4v}{8(1 - v)}, \quad S_{1122} = S_{2211} = \frac{4v - 1}{8(1 - v)}, \\
&S_{1133} = S_{2233} = \frac{v}{2(1 - v)}, \quad S_{1212} = \frac{3 - 4v}{4(1 - v)}, \\
&S_{1313} = S_{2323} = \frac{1}{2}.
\end{aligned} \tag{6}$$

And other components are zero. Substituting Eq. (6) into (5) yields

$$\begin{aligned}
&L_{1111} = L_{2222} = \frac{(1 - \alpha)(1 - v)(3 - 4v + 5\alpha - 4v\alpha)}{(1 + \alpha - 2v)(1 + 3\alpha - 4v\alpha)}, \\
&L_{1122} = L_{2211} = -\frac{(1 - \alpha)^2(1 - v)(1 - 4v)}{(1 + \alpha - 2v)(1 + 3\alpha - 4v\alpha)}, \\
&L_{1133} = L_{2233} = \frac{(1 - \alpha)^2 v}{(1 + \alpha - 2v)}, \quad L_{3333} = (1 - \alpha), \\
&L_{1212} = \frac{4(1 - \alpha)(1 - v)}{(1 + 3\alpha - 4v\alpha)}, \quad L_{1313} = L_{2323} = \frac{2(1 - \alpha)}{1 + \alpha}.
\end{aligned} \tag{7}$$

Other components of the $\mathbf{L}$ tensor are zero.

In our previous works, it was assumed that the size of the inclusion is small compared to the crack length and other dimensions of the crack body, and that the inclusion is located in the crack tip field controlled by the remotely applied SIF. For the present model shown in Fig. 1, the size of the inclusion may be so large such that it may be partially outside of the crack tip

field. In this case, we assumed that the stresses acting on the inclusion could be approximately expressed by

$$\sigma_{ij} \approx \frac{K_I^0}{\sqrt{2\pi r}}\tilde{\sigma}_{ij}(\theta) + \frac{K_{II}^0}{\sqrt{2\pi r}}\tilde{\tilde{\sigma}}_{ij}(\theta) + \sigma_{ij}^0. \tag{8}$$

The first and second terms are the crack tip fields which are applicable for $r \to 0$, and the third term is the remotely applied stress. When $r \to 0$ the remotely applied stresses are trivial compared to the singular crack tip stress, while for $r \to \infty$ the crack tip fields tend to be zero, the remotely applied stress is prevail. By using the well-known expressions of the crack tip stress field, the non-zero applied strains acting on the inclusion can be expressed by

$$\begin{aligned}
e_{11}^A &= \frac{K_I^0(1+\nu)}{E_m\sqrt{2\pi r}}\cos\frac{\theta}{2}\left[(1-2\nu) - \sin\frac{\theta}{2}\sin\frac{3\theta}{2}\right] \\
&\quad - \frac{K_{II}^0(1+\nu)}{E_m\sqrt{2\pi r}}\sin\frac{\theta}{2}\left[2(1-\nu) + \cos\frac{\theta}{2}\cos\frac{3\theta}{2}\right] + \frac{1-\nu^2}{E_m}\sigma_{11}^0 - \frac{\nu(1+\nu)}{E_m}\sigma_{22}^0, \\
e_{22}^A &= \frac{K_I^0(1+\nu)}{E_m\sqrt{2\pi r}}\cos\frac{\theta}{2}\left[(1-2\nu) + \sin\frac{\theta}{2}\sin\frac{3\theta}{2}\right] \\
&\quad + \frac{K_{II}^0(1+\nu)}{E_m\sqrt{2\pi r}}\sin\frac{\theta}{2}\left(2\nu + \cos\frac{\theta}{2}\cos\frac{3\theta}{2}\right) + \frac{1-\nu^2}{E_m}\sigma_{22}^0 - \frac{\nu(1+\nu)}{E_m}\sigma_{11}^0, \\
e_{12}^A &= \frac{(1+\nu)}{E_m\sqrt{2\pi r}}\cos\frac{\theta}{2}\left[K_I^0\sin\frac{\theta}{2}\cos\frac{3\theta}{2} + K_{II}^0\left(1 - \sin\frac{\theta}{2}\sin\frac{3\theta}{2}\right)\right] + \frac{(1+\nu)}{E_m}\sigma_{12}^0
\end{aligned} \tag{9}$$

for plane strain.

Substituting Eqs. (9) and (7) into (4) we have

$$\begin{aligned}
e_{11}^T &= \frac{(1-\alpha)(1-\nu)}{(1+\alpha-2\nu)(1+3\alpha-4\nu\alpha)}\left[(3-4\nu+5\alpha-4\nu\alpha)e_{11}^A - (1-\alpha)(1-4\nu)e_{22}^A\right], \\
e_{22}^T &= -\frac{(1-\alpha)(1-\nu)}{(1+\alpha-2\nu)(1+3\alpha-4\nu\alpha)}\left[(1-\alpha)(1-4\nu)e_{11}^A - (3-4\nu+5\alpha-4\nu\alpha)e_{22}^A\right], \\
e_{12}^T &= \frac{4(1-\alpha)(1-\nu)}{(1+3\alpha-4\nu\alpha)}e_{12}^A
\end{aligned} \tag{10}$$

for plane strain condition.

Based on the transformation toughening theory [17], [21], the enhancement in the SIFs for mode I and mode II cracks due to a transformed differential element of area dA are given by

$$dK_I^{tip} = \frac{1}{4\sqrt{2\pi}}\frac{E_m}{1-\nu^2}r^{-3/2}\Omega_1(e_{\alpha\gamma}^T, \theta)dA, \tag{11}$$

$$dK_{II}^{tip} = \frac{1}{16\sqrt{2\pi}}\frac{E_m}{1-\nu^2}r^{-3/2}\Omega_2(e_{\alpha\gamma}^T, \theta)dA, \tag{12}$$

where

$$\Omega_1(e_{\alpha\gamma}^T, \theta) = (e_{11}^T + e_{22}^T)\cos\frac{3\theta}{2} + 3e_{12}^T\cos\frac{5\theta}{2}\sin\theta + \frac{3}{2}(e_{22}^T - e_{11}^T)\sin\theta\sin\frac{5\theta}{2}, \tag{13}$$

$$\Omega_2(e_{\alpha\gamma}^T, \theta) = -(5e_{11}^T + 3e_{22}^T)\sin\frac{3\theta}{2} + 2e_{12}^T\left(3\cos\frac{7\theta}{2} + \cos\frac{3\theta}{2}\right) + 3(e_{22}^T - e_{11}^T)\sin\frac{7\theta}{2}. \tag{14}$$

Substituting Eqs. (10) and (13) into (11) and Eqs. (10) and (14) into Eq. (12), respectively, we have

$$\frac{dK_I^{tip}}{dA} = \frac{K_I^0}{\pi} r^{-2}\left(C_1 \cos\frac{\theta}{2}\cos\frac{3\theta}{2} + C_2 \sin^2\theta\cos\theta\right)$$
$$+ \frac{K_{II}^0}{\pi} r^{-2}\left[C_2 \sin\theta\left(1 - \frac{3}{2}\sin^2\theta\right) - \frac{C_1}{2}\sin\frac{\theta}{2}\cos\frac{3\theta}{2}\right]$$
$$+ \frac{1}{\sqrt{2\pi}} r^{-3/2}\left[C_1(\sigma_{11}^0 + \sigma_{22}^0)\cos\frac{3\theta}{2} + 2C_2\sin\theta\left((\sigma_{22}^0 - \sigma_{11}^0)\sin\frac{5\theta}{2} + 2\sigma_{12}^0\cos\frac{5\theta}{2}\right)\right], \quad (15)$$

$$\frac{dK_{II}^{\text{tip}}}{dA} = \frac{K_{II}^0}{\pi} r^{-2}\left(C_3\cos\theta - \frac{1}{4}C_1\cos 2\theta + \frac{3}{8}C_2\cos 3\theta\right)$$
$$+ \frac{K_I^0}{2\pi} r^{-2}\left[C_1\cos\frac{\theta}{2}\sin\frac{3\theta}{2} + \frac{1}{2}C_2\sin\theta\left(\cos 2\theta + \frac{1}{3}\right)\right]$$
$$+ \frac{1}{2\sqrt{2\pi}} r^{-3/2}\left[\left(-C_1(\sigma_{11}^0 + \sigma_{22}^0) + \frac{1}{3}(\sigma_{22}^0 - \sigma_{11}^0)\right)\sin\frac{3\theta}{2}\right.$$
$$\left. + C_2(\sigma_{22}^0 - \sigma_{11}^0)\sin\frac{7\theta}{2} + \frac{2}{3}C_2\sigma_{12}^0\left(\cos\frac{3\theta}{2} + 3\cos\frac{7\theta}{2}\right)\right], \quad (16)$$

where

$$C_1 = \frac{(1-\alpha)(1-2\nu)}{1+\alpha-2\nu},$$
$$C_2 = \frac{3(1-\alpha)}{2(1+3\alpha-4\nu\alpha)}, \quad (17)$$
$$C_3 = \frac{(1-\alpha)(11-22\nu+19\alpha-40\nu\alpha+32\nu^2\alpha)}{16(1+\alpha-2\nu)(1+3\alpha4\nu\alpha)}.$$

For the extreme case where E_i/E_m is either very large or zero, corresponding to a stiff inclusion or a hollow, we have

$$C_1 = 2\nu - 1, \quad C_2 = \frac{3}{4\nu-3}, \quad C_3 = \frac{19-40\nu+32\nu^2}{16(-3+4\nu)} \quad (\alpha\to\infty) \quad (18)$$

and

$$C_1 = 1, \quad C_2 = \frac{3}{2}, \quad C_3 = \frac{11}{16} \quad (\alpha = 0). \quad (19)$$

If the shape of the inclusion is known, the ΔK_I^{tip} and ΔK_{II}^{tip} can be calculated by

$$\Delta K_I^{tip} = \int_A dK_I^{tip} dA, \quad (20)$$

$$\Delta K_{II}^{tip} = \int_A dK_{II}^{tip} dA. \quad (21)$$

The integrals of Eqs. (20) and (21) extend over the area of the inclusion. As seen from Eqs. (15) and (16), there is a coupling effect between mode I and mode II loads when the inclusion is unsymmetric with respect to the crack line.

3 Numerical examples and discussion

Two basic assumptions have been used in the previous derivations: one is that the Eshelby inclusion theory can be approximately used for each differential element in an inclusion, such that this theory can be extended to an inclusion of arbitrary shape; the other is that the stresses acting on the inclusion are approached by Eq. (8), which is accurate only when the distance between the inclusion and the crack tip is either very large or very small. Although the former has been validated by a number of numerical examples in our previous studies [15]–[17], the latter assumption is still to be substantiated. Hence, in the following numerical examples, the size of the inclusion is chosen in the same order as the crack length. The validations of the present solutions are performed by detailed finite element analysis. The details for the calculation of the crack tip SIF by FE-analysis were described in our previous works [15], [16]. In the following, the crack tip SIFs calculated from the present solution and the FE-analysis are normalized by the remotely applied SIF, which is the SIF in the absence of an inclusion for the crack body subjected to the same remotely applied load.

Figure 2 shows a center-crack plane with a rectangular inclusion symmetrics with respect to the crack line under biaxial tension loadings ($\sigma_{11}^0 = \sigma_{22}^0$). In this case, only mode I SIF is present and Eq. (20) reduces to

$$\Delta K_I^{tip} = \frac{K_I^0}{\pi} \int_A \left\{ r^{-2} \left(C_1 \cos\frac{\theta}{2} \cos\frac{3\theta}{2} + C_2 \sin^2\theta \cos\theta \right) + \frac{1}{\sqrt{2\pi}} r^{-3/2} \left[C_1 (\sigma_{11}^0 + \sigma_{22}^0) \cos\frac{3\theta}{2} \right] \right\} dA. \tag{22}$$

The first term is the result obtained by Li and Chen [16], representing the effect of the crack tip field; the second term represents the influence of the remotely applied stresses on the crack tip SIF. As shown in Fig. 2, the agreement between the prediction of (22) and the FE-analyses is fairly good. The results of (22) in the absence of the second term are also displayed. As shown in Fig. 2, the predicting accuracy of (22) is improved due to the introduction of the remotely applied stresses.

Figure 3 displays the interaction between a crack and a hard circular inclusion ($\alpha = 2$) under pure mode II loading. Then Eq. (21) reduces to

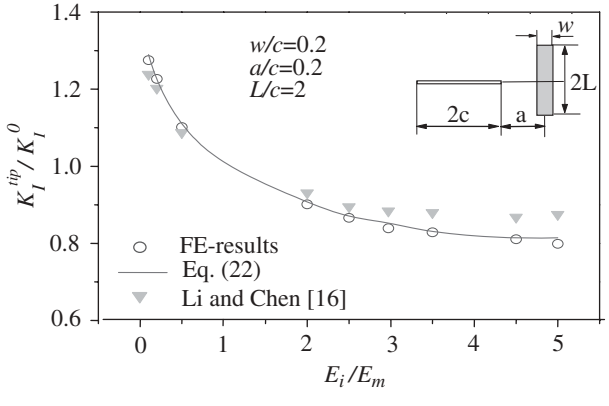

Fig. 2. The interaction between a crack and a rectangular inclusion under biaxially tensile loading ($\sigma_{11}^0 = \sigma_{22}^0, \sigma_{12}^0 = 0$) as a function of the modulus ratios

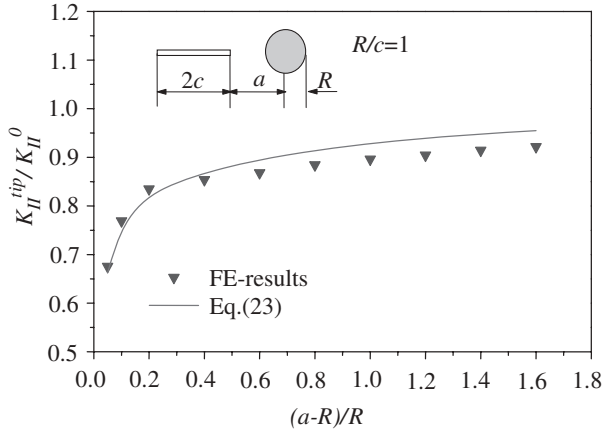

Fig. 3. The interaction between a crack and a hard circular inclusion ($\alpha = 2$) under pure mode II loading as a function of the distance between the crack tip and the inclusion

$$\Delta K_{II}^{\text{tip}} = \frac{K_{II}^{0}}{\pi}\int_{A} r^{-2}\left(C_3\cos\theta - \frac{1}{4}C_1\cos 2\theta + \frac{3}{8}C_2\cos 3\theta\right)dA$$
$$+ \frac{1}{3\sqrt{2\pi}}C_2\sigma_{12}^{0}\int_{A} r^{-3/2}\left(\cos\frac{3\theta}{2} + 3\cos\frac{7\theta}{2}\right)dA. \tag{23}$$

The first term is the result obtained by Yang et al. [17], representing the effect of the crack tip field; the second term represents the influence of the remotely applied stresses σ_{12}^{0} on the crack tip SIF. As shown in Fig. 3, when the crack approaches the hard inclusion, the near tip SIF decreases remarkably. The predictions of Eq. (23) are also in good agreement with the FE-results.

Figure 4 shows an infinite plane containing a circular inclusion and a crack subjected to far-field tension perpendicular to the line connecting the centers of the inclusion and the crack. The normalized mode I and mode II SIFs for crack tip A calculated from (20) and (21) for a hard inclusion ($\alpha = 2$) as functions of the crack orientation angle θ are shown in Fig. 5, and as functions of the modulus ratio are shown in Fig. 6 for fixed crack orientation angle ($\theta = 60^0$).

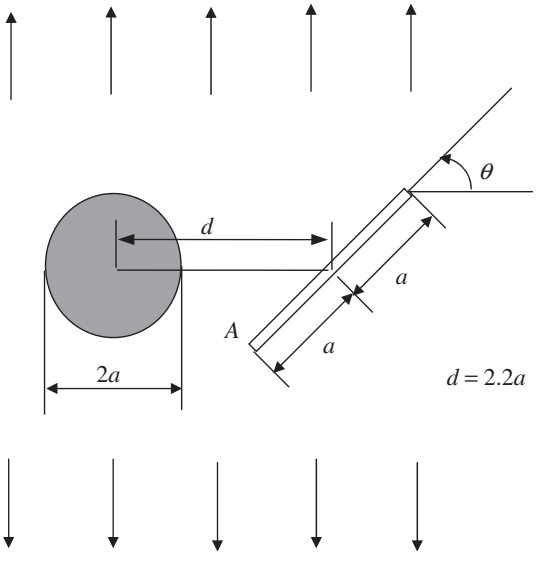

Fig. 4. A circular inclusion and an inclined crack subject to far-field tension

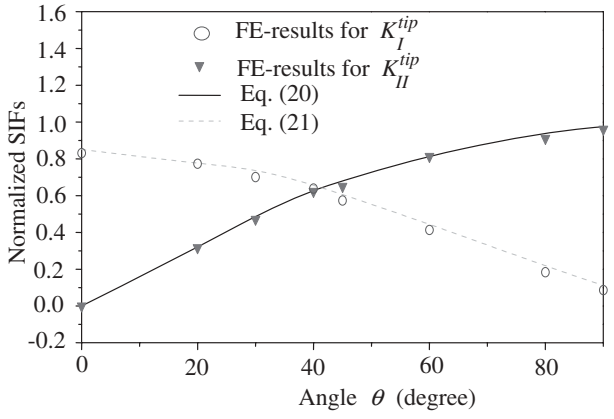

Fig. 5. The normalized SIFs (near the crack tip A) for the model shown in Fig. 4 as functions of the crack incline angle θ at fixed modulus ratio $\alpha = 2$

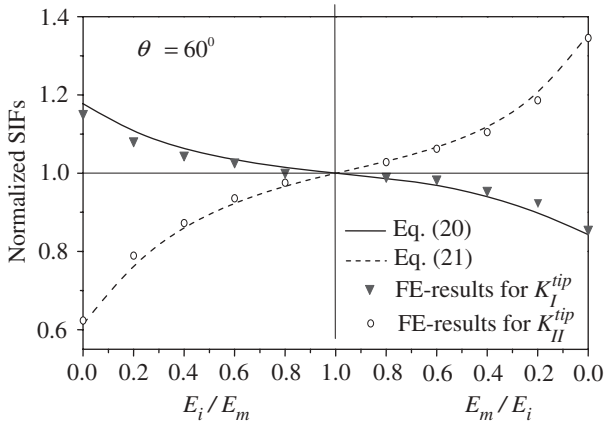

Fig. 6. The normalized SIFs (near the crack tip A) for the model shown in Fig. 4 as functions of the modulus ratios at fixed crack incline angle $\theta = 60^0$

As compared with the corresponding FE-results, all the results shown in Figs. 5 and 6 appear to be in good agreement. Note that the K_I^{tip} and K_{II}^{tip} in Figs. 5 and 6 are normalized by K_I^0, which is the SIF for the crack orientation angle $\theta = 0$ in the absence of the inclusion.

4 Conclusions

A generally applicable approximation solution is developed to predict the interaction between I/II mixed-mode crack and an inclusion. As validated by detailed finite element analyses, the present solution has good accuracy for the inclusion of arbitrary shape and large size due to introducing the effect of the remotely applied stresses on the inclusion. For the inclusion with small size and located in the crack tip field, the present solution reduces to the existing one.

Acknowledgements

The financial supports from National Basic Research Program of China through Grant No. 2004CB619303 and from the National Science Foundation of China under Grant No.10572088 are gratefully acknowledged.

References

[1] Atkinson, C.: The interaction between a crack and an inclusion. Int. J. Engng. Sci. **10**, 127–136 (1972).
[2] Erdogan, F., Gupta, G. D., Ratwani, M.: Interaction between a circular inclusion and an arbitrary oriented crack. J. Appl. Mech. **41**, 1007–1013 (1974).
[3] Lam, K. Y., Ong, P. P., Wude, N.: Interaction between a circular inclusion and a symmetrically branched crack. Theor. Appl. Fract. Mech. **28**, 197–21 (1998).
[4] Patton, E. M., Santare, M. H.: The effect of a rigid elliptical inclusion on a straight crack. Int. J. Fracture **46**, 71–79 (1990).
[5] Chen, A. H.: The effect of an elliptical inclusion on a crack. Int. J. Fracture **85**, 351–364 (1997).
[6] Lipetzky, P., Schmauder, S.: Crack-particle interaction in two-phase composites, Part I: Particle shape effects. Int. J. Fracture **65**, 345–358 (1994).
[7] Lipetzky, P., Knesl, Z.: Crack-particle interaction in two-phase composites, Part II: Crack Deflection. Int. J. Fracture **73**, 81–92 (1995).
[8] Stam, G. T. M., Giessen, E. Van Der, Meuers, P.: Effect of transformation-induced shear strains on crack growth in zirconia-containing ceramics. Int. J. Solids Struct. **31**, 1923–1948 (1994).
[9] Thomas, S. B., Mhaiskar, M. J., Sethuraman R.: Stress intensity factors for circular hole and inclusion using finite element alternating method. Theor. Appl. Fract. Mech. **33**, 73–81 (2000).
[10] Portela, A., Aliabadi, M. H., Rooke, D. P.: Dual boundary element integral analysis of crack propagation. Composites Struct. **46**, 237–247 (1993).
[11] Bush, M. B.: The Interaction between a crack and a particle cluster. Int. J. Fracture **88**, 215–232 (1997).
[12] Wang, C., Libardi, N., Baldo, J. B.: Analysis of crack extension paths and toughening in a two phase brittle particulate composites by the boundary element method. Int. J. Fracture **94**, 177–188 (1998).
[13] Tamate, O.: The effect of a circular inclusion on the stresses around a line crack in a sheet under tension. Int. J. Fracture **4**, 257–266 (1968).
[14] Helsing, J.: Stress intensity factors for a crack in front of an inclusion. Engng. Fract. Mech. **64**, 245–253 (1999).
[15] Li, Z., Yang, L.: The near-tip stress intensity factor partially penetrating an inclusion. J. Appl. Mech. **71**, 465–470 (2004).
[16] Li, Z., Chen, Q.: Crack-inclusion interaction for mode I crack analyzed by Eshelby equivalent inclusion method. Int. J. Fracture **118**, 29–40 (2002).
[17] Yang, L., Chen, Q., Li, Z.: Crack-inclusion interaction for mode II crack analyzed by Eshelby equivalent inclusion method. Engng. Fract. Mech. **71**, 1421–1433 (2004).
[18] Eshelby, J. D.: The determination of the elastic fields of an ellipsoidal inclusion and related problems. Proc. Royal Soc. London, Series A, **241**, 376–396 (1957).
[19] Withers, P. J., Stobbs, W. M., Pederson, O. B.: The application of the Eshelby method of internal stress determination to short fiber metal matrix composites. Acta Metall. **37**, 3061–3084 (1989).
[20] Mura, T.: Micromechanics of defects in solids, 2nd rev. ed. Dordrecht 1987.
[21] Lambropoulos, J. C.: Shear, shape and orientation effects in transformation toughening in ceramics. Int. J. Solids Struct. **22**, 1083–1106 (1986).

Authors' addresses: Z. Li and Q. Sheng, School of Naval Architecture, Ocean and Civil Engineering, Shanghai Jiaotong University (E-mail: zhli@sjtu.edu.cn); J. Sun, State Key Laboratory for Mechanical Behavior of Materials, School of Materials Science and Engineering, Xi'an Jiaotong University, P. R. China